THE JOURNAL OF BIOLOGICAL CHEMISTRY VOL. 284, NO. 21, pp. 14359–14367, May 22, 2009

The Rate-limiting Step in the Cytochrome bc_1 Complex (Ubiquinol-Cytochrome *c* Oxidoreductase) Is Not Changed by Inhibition of Cytochrome *b*-dependent Deprotonation

IMPLICATIONS FOR THE MECHANISM OF UBIQUINOL OXIDATION AT CENTER P OF THE bc_1 COMPLEX[*][S]

Received for publication, March 4, 2009, and in revised form, March 17, 2009 Published, JBC Papers in Press, March 26, 2009, DOI 10.1074/jbc.M109.000596

Raul Covian and Bernard L. Trumpower[1]

From the Department of Biochemistry, Dartmouth Medical School, Hanover, New Hampshire 03755

Quinol oxidation at center P of the cytochrome bc_1 complex involves bifurcated electron transfer to the Rieske iron-sulfur protein and cytochrome *b*. It is unknown whether both electrons are transferred from the same domain close to the Rieske protein, or if an unstable semiquinone anion intermediate diffuses rapidly to the vicinity of the b_L heme. We have determined the pre-steady state rate and activation energy (E_a) for quinol oxidation in purified yeast bc_1 complexes harboring either a Y185F mutation in the Rieske protein, which decreases the redox potential of the FeS cluster, or a E272Q cytochrome *b* mutation, which eliminates the proton acceptor in cytochrome *b*. The rate of the bifurcated reaction in the E272Q mutant (<10% of the wild type) was even lower than that of the Y185F enzyme (~20% of the wild type). However, the E272Q enzyme showed the same E_a (61 kJ mol^{-1}) with respect to the wild type (62 kJ mol^{-1}), in contrast with the Y185F mutation, which increased E_a to 73 kJ mol^{-1}. The rate and E_a of the slow reaction of quinol with oxygen that are observed after cytochrome *b* is reduced were unaffected by the E272Q substitution, whereas the Y185F mutation modified only its rate. The Y185F/E272Q double mutation resulted in a synergistic decrease in the rate of quinol oxidation (0.7% of the wild type). These results are inconsistent with a sequential "movable semiquinone" mechanism but are consistent with a model in which both electrons are transferred simultaneously from the same domain in center P.

The cytochrome bc_1 complex couples the oxidation of a two-electron carrier molecule of quinol to the movement of protons across the inner mitochondrial or bacterial membrane. The key reaction in this energy-conserving mechanism, known as the Q-cycle (1, 2), is the bifurcation of electrons at the active site located closer to the positive side of the membrane, termed center P or Q_o site. One of the electrons from quinol is transferred to a chain of one-electron carriers with relatively high redox potentials that include the FeS cluster of the Rieske protein and the hemes of cytochromes c_1 and *c*. The other electron is donated to the low potential (b_L) heme of cytochrome *b*, from which it crosses most of the membrane width to the high potential b_H heme, located close to another active site (center N or Q_i site), where quinone is reduced to quinol after two center P turnovers. Proton release and uptake at each active site are achieved by taking advantage of the chemistry of quinol and quinone, which can only stably exist at physiological pH in the protonated and deprotonated forms, respectively.

Critical to the electron bifurcation reaction at center P is the arrangement of protonatable groups (His^{181} of the Rieske protein and Glu^{272} of cytochrome *b*) close to the electron acceptors at opposite sides of the substrate (see Fig. 1). However, the exact mechanism of electron bifurcation at center P is still an unresolved issue. Proposed models have ranged from strictly concerted mechanisms in which both electrons from quinol are extracted simultaneously (3, 4) to those that postulate a highly stabilized semiquinone intermediate (5). Between these two extremes are mechanisms that propose the formation of an unstable semiquinone intermediate after a first electron transfer from quinol to the Rieske protein (6–8), which seem to be supported by recent reports that claim to have detected low concentrations of semiquinone at center P when reoxidation of cytochrome *b* is impeded under special conditions (9, 10). One version of the unstable semiquinone mechanism proposes that this intermediate diffuses from the vicinity of the Rieske protein to a location within center P located closer to the b_L heme, which would allow non-rate-limiting rates of b_L reduction to occur even at very low semiquinone occupancy (11). In this proposal, the movement of the unstable semiquinone would be allowed by protonation and rotation of Glu^{272} in cytochrome *b*, which occupies different conformations in crystallographic structures (Fig. 1) (11–14).

An important prediction of the movable semiquinone model (11) is that mutation of Glu^{272} should impede diffusion of the anionic semiquinone, forcing electron transfer to the b_L heme to occur through a longer distance from the position closer to the Rieske FeS cluster (15), thereby shifting the rate-limiting step from the first to the second electron transfer. Although it has already been reported that different mutations at Glu^{272} partially slow down quinol oxidation at center P (15–17), no effort has been made so far to evaluate whether the rate-limiting step changes upon inhibition of the deprotonation of quinol (or of a putative semiquinone intermediate) by mutation of the

* This work was supported, in whole or in part, by National Institutes of Health Research Grant GM 20379.

[S] The on-line version of this article (available at http://www.jbc.org) contains supplemental data.

[1] To whom correspondence should be addressed: Dept. of Biochemistry, Dartmouth Medical School, 7200 Vail, Hanover, NH 03755. Tel.: 603-650-1621; Fax: 603-650-1128; E-mail: Trumpower@Dartmouth.edu.

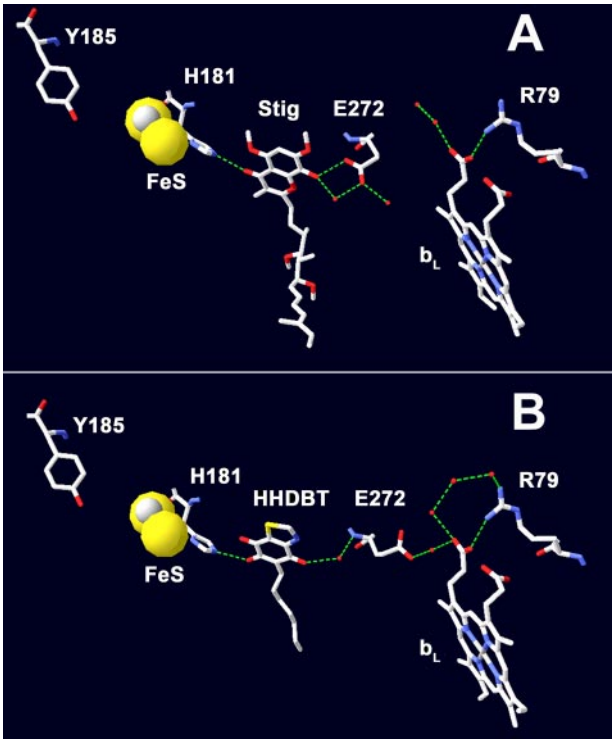

FIGURE 1. **Electron and proton acceptors involved in quinol oxidation at center P.** Crystallographic structures 1EZV (12) and 1P84 (13) show stigmatellin (*A*) or 5-*n*-heptyl-6-hydroxy-4,7-dioxobenzothiazole (*B*) bound at center P forming a hydrogen bond to the His^{181} residue of the Rieske protein, which is a ligand to the FeS cluster. The Tyr^{185} residue in the Rieske protein influences the E_m value of the FeS cluster (22). On the side pointing to the b_L heme, a bound water molecule is also hydrogen-bonded to the inhibitor, either to the Glu^{272} carboxylate in cytochrome *b* (*A*), or to its backbone amino group (*B*), when the side chain is rotated toward a water network that connects to the propionate of the b_L heme and to Arg^{79} of cytochrome *b*.

cytochrome *b* Glu^{272}. In the present work, we analyze the energy of activation of quinol oxidation at center P and show that the rate-limiting step when Glu^{272} is mutated to glutamine, although slower, is still determined by the driving force for electron transfer to the Rieske protein. We also show that decreasing this driving force enhances the relative inhibition caused by mutating Glu^{272}, suggesting a tight coupling of reactions involved in quinol oxidation and deprotonation. In contrast, reactions with oxygen that bypass the electron bifurcation at center P, which are likely to involve a semiquinone intermediate, are independent of Glu^{272} and go through an energetic barrier different from that of the bifurcated reaction. We discuss how these results support a mechanism in which both electron transfer events from quinol to the Rieske protein and the b_L heme occur from the same position and at the same time.

EXPERIMENTAL PROCEDURES

Materials—Dodecyl maltoside was obtained from Anatrace. DEAE-Bio-Gel A was from Bio-Rad. Stigmatellin, antimycin, and decylubiquione were purchased from Sigma. Decylubiquinol (2,3-dimethoxy-5-methyl-6-decyl-1,4-benzoquinol; DBH_2)[2] was prepared from decylubiquione as described (18) and quantified by UV spectroscopy using an extinction coefficient of 4.14 mM^{-1} cm^{-1} at 290 nm (19). Inhibitors were dissolved in ethanol and quantified by UV spectroscopy (20) using extinction coefficients of 4.8 mM^{-1} cm^{-1} at 320 nm for antimycin and 65.5 mM^{-1} cm^{-1} at 267 nm for stigmatellin (21).

Yeast Strains—Haploid yeast strains containing either the gene for the wild type or Y185F Rieske protein in the single-copy plasmid pEDRIP1 (22) and the wild type or the E272Q intronless cytochrome *b* gene introduced by biolistic transformation (16) were obtained from Dr. Brigitte Meunier (Centre de Génétique Moléculaire, CNRS, Gif, France). All strains were grown in YPD medium (1% yeast extract, 2% Bacto-peptone, and 2% dextrose) and grown under aeration to late exponential phase.

Purification of Cytochrome bc_1 Complex—Cytochrome bc_1 complex was isolated from each yeast strain as described previously (23), except that the dodecyl maltoside concentration was increased to 0.05% in the elution buffers, and the volume of DEAE-Bio-Gel A was reduced to 25 ml to increase the yield of active enzyme. Quantification of the bc_1 complex was performed as described (24) using extinction coefficients of 17.5 mM^{-1} cm^{-1} at 553–539 nm for cytochrome c_1 (25) and 25.6 mM^{-1} cm^{-1} at 563–579 nm for the average absorbance of the b_H and b_L hemes in cytochrome *b* (26, 27).

Determination of the Energy of Activation (E_a)—Pre-steady state reduction of cytochromes *b* and *c* was followed at room temperature by stopped flow rapid scanning spectroscopy using the Olis rapid scanning monochromator as described (24). The temperature of the mixing chamber was varied from 10–30 °C with a thermostatically controlled Julabo F12 circulating water bath, and the temperature of the enzyme sample was equilibrated to that of the mixing chamber before each reaction. Reactions were started by mixing 1 μM cytochrome bc_1 complex, 1.5 μM antimycin (to inhibit center N), 1 mM KCN (to inhibit the contaminating cytochrome *c* oxidase), and 10 μM horse heart cytochrome *c* in assay buffer containing 50 mM potassium phosphate, pH 7.0, plus 1 mM sodium azide, 1 mM EDTA, and 0.05% Tween 20 against an equal volume of the same buffer containing 20–320 μM DBH_2. For each experiment, six to eight data sets were averaged after subtracting the oxidized spectrum. The time course of absorbance changes at 563–579 nm (cytochrome *b*) and 550–539 nm (cytochrome *c*) was extracted using software from Olis and exported to the Origin 5.0 program (OriginLab Corp.), where kinetic traces were fitted to two or three component exponential functions, as appropriate.

The initial rates obtained from cytochromes *b* and *c* reduction traces were very similar to each other and corresponded to the rate of bifurcated quinol oxidation. The final slow reduction of cytochrome *c* observed after the completion of cytochrome *b* reduction was fitted to a straight line, and the value of the slope was divided by the extinction coefficient for cytochrome *c*, which is 21.5 mM^{-1} cm^{-1} (28), to obtain the turnover rate for the non-bifurcated oxidation of quinol. Rates obtained at the same DBH_2 concentration were plotted as a function of temperature according to the Arrhenius equation and fitted to a straight line to obtain E_a values.

Kinetic Modeling—The DynaFit program (BioKin, Ltd.), which allows the simulation of reaction mechanisms described

[2] The abbreviations used are: DBH_2, decylubiquinol (2,3-dimethoxy-5-methyl-6-decyl-1,4-benzoquinol).

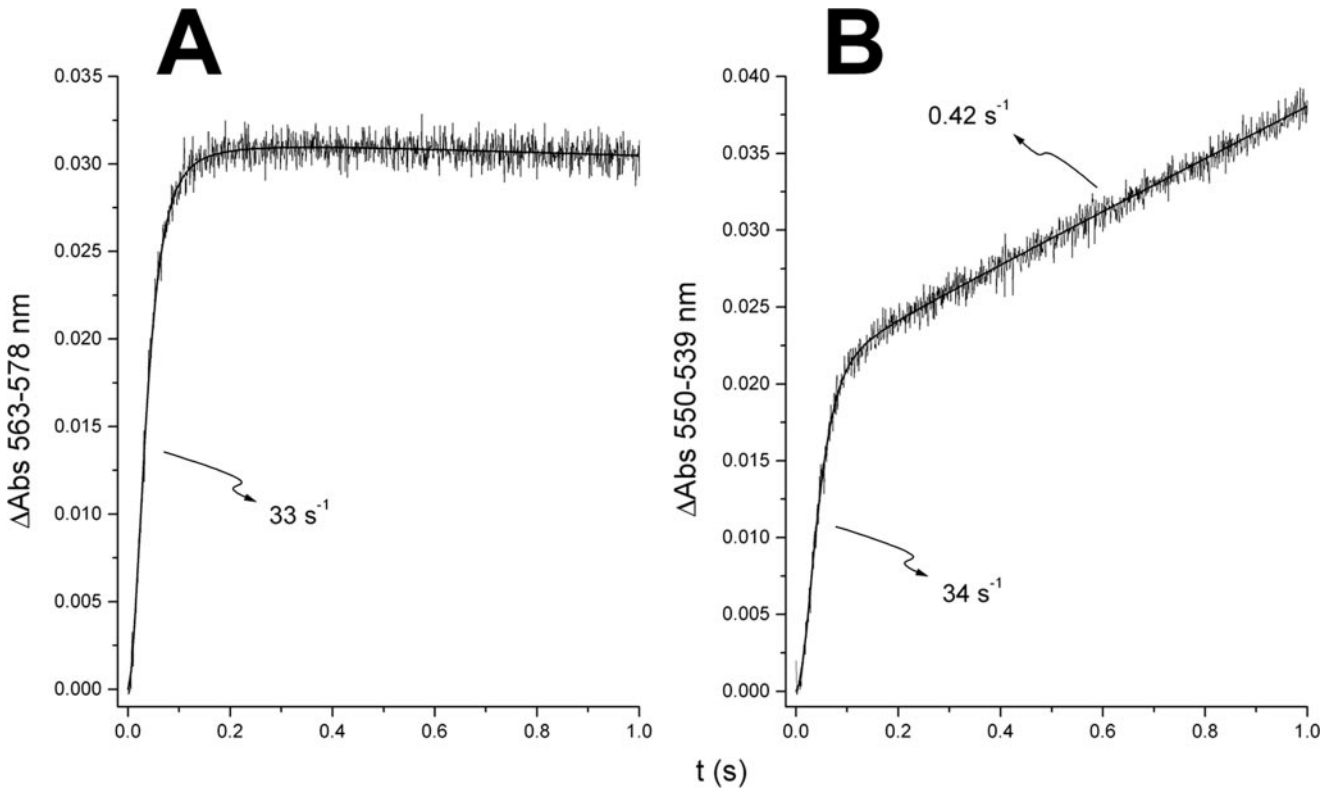

FIGURE 2. **Pre-steady state oxidation of DBH_2 by the wild-type bc_1 complex.** Reduction of cytochrome *b* (*A*) and cytochrome *c* (*B*) were followed at the indicated wavelength pairs after rapid mixing of 1 μM purified bc_1 complex and 10 μM horse heart cytochrome *c* with 160 μM DBH_2 at 20 °C. *Solid lines* correspond to the best fit of each trace to a double exponential function from which the indicated initial reduction rates were obtained. The beginning of the second phase of cytochrome *c* reduction (*B*) was fitted to a straight line to calculate the indicated turnover rate for the slower process.

as a series of individual reaction steps (29), was used to simulate the rate of cytochrome *b* reduction and the relative concentration of semiquinone intermediate expected from a sequential mechanism that allows movement of semiquinone close to the b_L heme. The model used (see supplemental data for the full DynaFit script) assumed an almost complete saturation of center P with substrate (200 μM quinol with a K_m of 10 μM) with the subsequent formation and consumption of semiquinone occurring at the rates suggested in Ref. 15. The one-electron oxidation of quinol by the Rieske protein (k_1) was assumed to occur with a forward rate of 1.3×10^3 s^{-1}, whereas the rates of the second electron transfer from semiquinone to the b_L heme were 1.9×10^7 s^{-1} from the position distal to the heme (k_{2d}), and 1.9×10^{11} s^{-1} from the proximal position (k_{2p}). Reverse electron transfer rates (k_{-1}, k_{-2d}, and k_{-2p}) were set to appropriate values with respect to the forward rates to yield a K_{eq} of 4×10^{-8}, and the rate of semiquinone diffusion from the distal to the proximal domain (k_{diff}) was varied and considered to be reversible. Dissociation of the quinone (k_{off}) product from either of the two domains was also included, with a rate identical to that for quinol but with a 10-fold lower binding rate (k_{onQ}), as suggested by the higher affinity of center P for quinol (6).

RESULTS

Effect of the Y185F and E272Q Mutations on the Rates of Quinol Oxidation at Center P—In the presence of antimycin and cytochrome *c*, the bifurcated oxidation of DBH_2 was evidenced by the simultaneous reduction of cytochromes *b* and *c*, which occurred at the same rate, as shown in the representative experiments of Fig. 2. After two turnovers, reduction of cytochrome *b* equivalent to the full absorbance of the b_H hemes was accomplished (Fig. 2*A*), along with the reduction of two equivalents of cytochrome *c* (Fig. 2*B*). The highly reduced state of cytochrome *b* prevented additional bifurcation of the electrons from DBH_2, resulting in further oxidation of the substrate at a much slower rate (1–2% of the bifurcated reaction rate) and evidenced as a second, practically linear phase of cytochrome *c* reduction (Fig. 2*B*) without a corresponding reduction in cytochrome *b*. As we have reported previously (30), this slow reduction of cytochrome *c* is partially (30–40%) inhibited by Mn-superoxide dismutase, indicating that it corresponds to the "bypass" reaction at center P in which the one-electron reduction of quinol by the Rieske protein forms an unstable semiquinone that can either react with oxygen to form superoxide or receive an electron from b_L to reform quinol (31). An advantage of this pre-steady state method of measuring quinol oxidation at center P is that both the bifurcated and bypass reactions can be determined in the same kinetic trace in a time scale of milliseconds, which virtually eliminates any contribution from the non-enzymatic oxidation of the quinol analog. In contrast, steady state measurements require separate experiments in the presence and absence of antimycin, different enzyme concentrations in the nM range, and collection times in tens of seconds that greatly increase the contribution of the chemical reduction

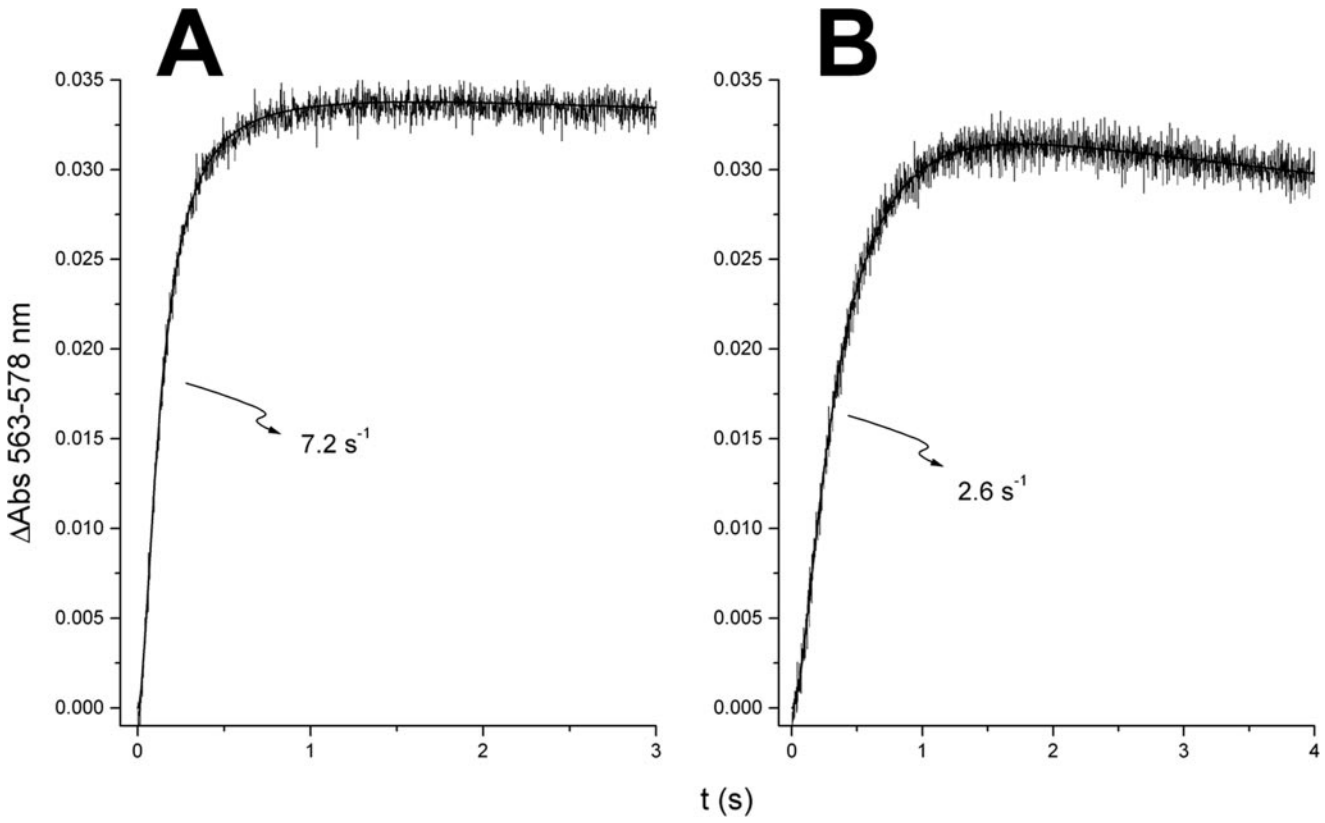

FIGURE 3. **Pre-steady state reduction of cytochrome *b* by DBH_2 in bc_1 complexes with single mutations.** Absorbance (*Abs*) change kinetics at the indicated wavelength pair were obtained by mixing 10 μM cytochrome *c* and 1 μM bc_1 complex containing the Y185F substitution in the Rieske protein (*A*) or the E272Q mutation in cytochrome *b* (*B*) with 160 μM DBH_2 at 20 °C. *Solid lines* correspond to the best fit of each trace to a double (*A*) or triple (*B*) exponential function from which the indicated initial reduction rates were obtained.

of cytochrome *c* with respect to the enzymatic rate, especially when measuring the slow bypass reactions (32).

The Y185F mutation at the Rieske protein decreases the redox potential of the Rieske cluster by at least 60 mV, resulting in a decreased driving force for quinol oxidation and consequently a slower rate (22). The E272Q substitution in cytochrome *b* decreases the rate by eliminating a potential proton acceptor but without altering the midpoint potential of any redox groups (16). As shown in Fig. 3, the E272Q mutation in cytochrome *b* inhibited the bifurcated oxidation of DBH_2 to a larger extent (~8% of the wild-type rate in Fig. 2) than the Y185F mutation in the Rieske protein (22% of the wild type). The absorbance at the wavelengths used to report cytochrome *b* reduction showed a slight decrease in the E272Q mutant (Fig. 3*B*). We found that this effect was due to a negative spectral contribution of cytochrome *c* reduction at that wavelength pair and not to an actual reoxidation of cytochrome *b* (data not shown). This suggested a faster reduction of cytochrome *c* after the completion of the bifurcated reaction in the E272Q enzyme. This was indeed the case, as shown in Fig. 4. The Y185F mutation decreased the rates for both the bifurcated and bypass reactions relative to the wild-type enzyme (Fig. 4*A*) while retaining a proportion of ~2% between the rates of both processes. In contrast, the non-bifurcated oxidation of quinol linked to superoxide anion formation was not inhibited at all by the E272Q substitution relative to the wild type (Fig. 4*B*), with the rate for this process (0.46 s^{-1}) being 18% relative to the rate of the bifurcated reaction. This agrees with the significant inhibition of the steady state activity of this mutant by superoxide dismutase reported even in the absence of antimycin (16), as well as with the unaltered bypass reaction relative to the wild-type enzyme by the equivalent mutation E295Q in the bacterial bc_1 complex (15).

Because each of the mutations that we are characterizing is present in a different subunit on opposite sides of center P and because each decreases the rate of quinol oxidation by a different mechanism, it is reasonable to expect that they should have additive effects when simultaneously present in the bc_1 complex. However, as shown in Fig. 5, a synergistic effect was obtained in the Y185F/E272Q double mutant. A purely additive effect of each mutation should have yielded a bifurcated rate of ~0.6 s^{-1}, calculated from the 8% (relative rate obtained in the E272Q single mutant) of 7.2 s^{-1} (rate obtained with the Y185F mutant) (see Fig. 3). The actual rate of the double mutant was 3-fold lower than the predicted value based on cytochrome *b* kinetics (Fig. 5*A*) and resulted in equal rates for the bifurcated and bypass reactions as observed in the reduction of cytochrome *c* (Fig. 5*B*). This latter effect was due mainly to the synergistic decrease in the rate of the bifurcated reaction by the two mutations because the rate of the bypass was not very different from that obtained in the Y185F single mutant (compare with Fig. 4*A*). This relatively high rate for cytochrome *c* reduction accounts for the marked decrease of absorbance observed at the wavelength pair used to monitor cytochrome *b* (Fig. 5*A*).

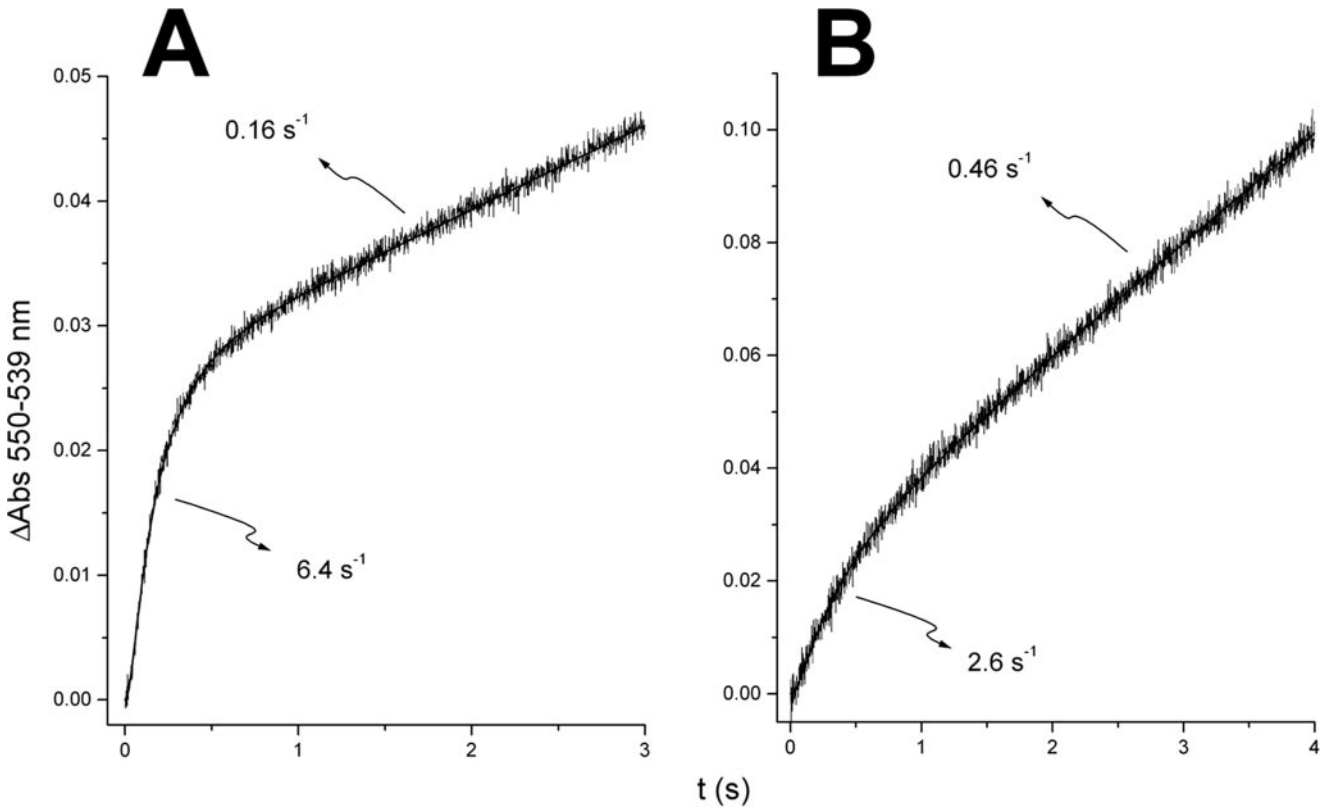

FIGURE 4. **Pre-steady state reduction of cytochrome *c* by DBH_2 in bc_1 complexes with single mutations.** Absorbance (*Abs*) change kinetics at the indicated wavelength pair were obtained by mixing 10 μM cytochrome *c* and 1 μM bc_1 complex containing the Y185F substitution in the Rieske protein (*A*) or the E272Q mutation in cytochrome *b* (*B*) with 160 μM DBH_2 at 20 °C. *Solid lines* correspond to the best fit of each trace to a double exponential function from which the indicated initial reduction rate was obtained. The beginning of the second phase was fitted to a straight line to calculate the indicated turnover rate for the slower reduction.

Nevertheless, after correction for this spurious spectral contribution, the extent of cytochrome *b* reduction stabilized at a level of only 50% of that observed in the wild type or in the single mutants (data not shown), which can be explained as an effect of the bypass reaction competing for electrons that would normally be accumulated in cytochrome *b* by the bifurcated process.

Effect of the Y185F and E272Q Mutations on the Energy of Activation at Center P—Rates of reduction of cytochromes *b* and *c* obtained at different temperatures and DBH_2 concentrations were used to determine the values of the activation energy (E_a) for the reactions occurring at center P. E_a values are ideally determined under conditions of substrate saturation to avoid the interference from temperature-dependent changes in the affinity of the active site. However, the time resolution of the rapid scanning monochromator used (1 scan/ms) would result in significant inaccuracies in trying to determine rates >150 s^{-1}, which would still be lower than the V_{max} for center P in yeast (27). Therefore, we used a detergent concentration in the assay buffer appropriate to achieve under-saturation of center P by DBH_2 ($K_m \sim 150$ μM) that would yield lower oxidation rates. This experimental approach was validated by the observation that the E_a values obtained at each DBH_2 concentration were within 5% of those obtained at the other DBH_2 concentrations, with no shift to higher or lower values as the substrate concentration was increased.

The reported critical micellar concentration of Tween 20 is 0.006% at 25 °C (33) and is expected to decrease slightly at lower temperatures (34). Because the concentration of Tween 20 used in our assay buffer (0.05%) was much higher than the critical micellar concentration, we can discard changes in the effective detergent concentration at the different temperatures tested, as validated by the linear behavior of the Arrhenius plots we obtained.

As shown in Fig. 6, the average E_a value for the bifurcated reaction, as calculated from the rates of cytochrome *b* reduction (Fig. 6*A*), was slightly higher than for the slow phase of cytochrome *c* reduction, which reports the bypass reaction (Fig. 6*B*). The E_a for the bifurcated reaction obtained from the first fast phase of cytochrome *c* reduction (see Fig. 2*B*) was within the range obtained with cytochrome *b* (65 ± 4 kJ mol^{-1}) but had a higher uncertainty at faster rates because of the presence of the second kinetic phase, which increased the error in the fitting of the first phase (data not shown). In addition, the K_m for the bypass reaction was significantly higher than for the bifurcated reaction, as can be seen from the increased separation in the data points corresponding to the two highest DBH_2 concentrations in Fig. 6*B* relative to those in Fig. 6*A*.

A decrease in the catalytic rate of an enzymatic reaction by a mutation can have the consequence of increasing the activation energy of the rate-limiting step, or it can slow down another reaction in the catalytic cycle to the point that a new rate-lim-

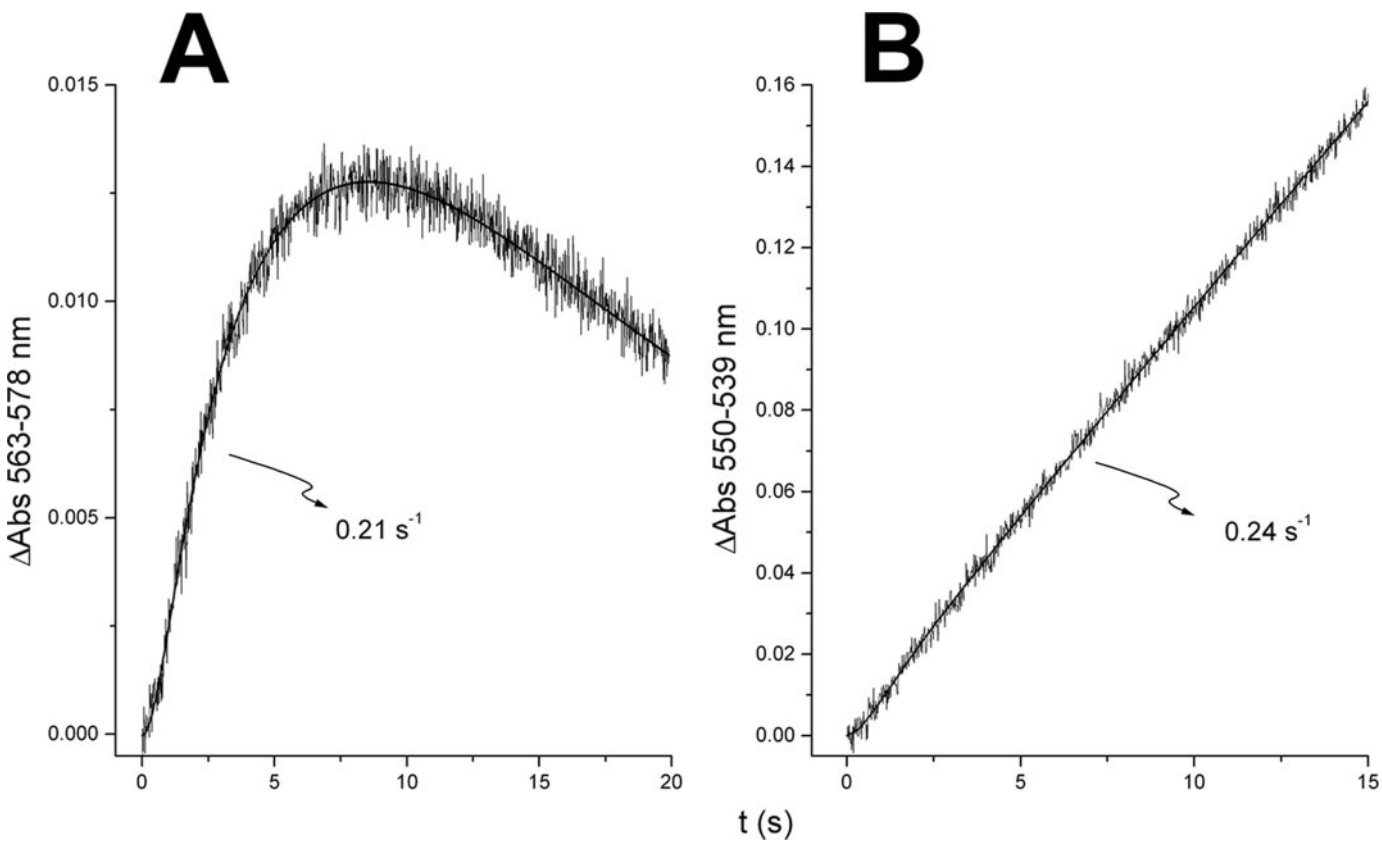

FIGURE 5. **Pre-steady state oxidation of DBH_2 by the Y185F/E272Q double mutant bc_1 complex.** Reduction of cytochrome *b* (*A*) and cytochrome *c* (*B*) were followed at the indicated wavelength pairs after rapid mixing of 10 μM horse heart cytochrome *c* and 1 μM purified bc_1 complex containing both the Y185F and E272Q substitutions with 160 μM DBH_2 at 20 °C. *Solid lines* correspond to the best fit of each trace to a double (*A*) exponential or single (*B*) function from which the indicated reduction rates were obtained.

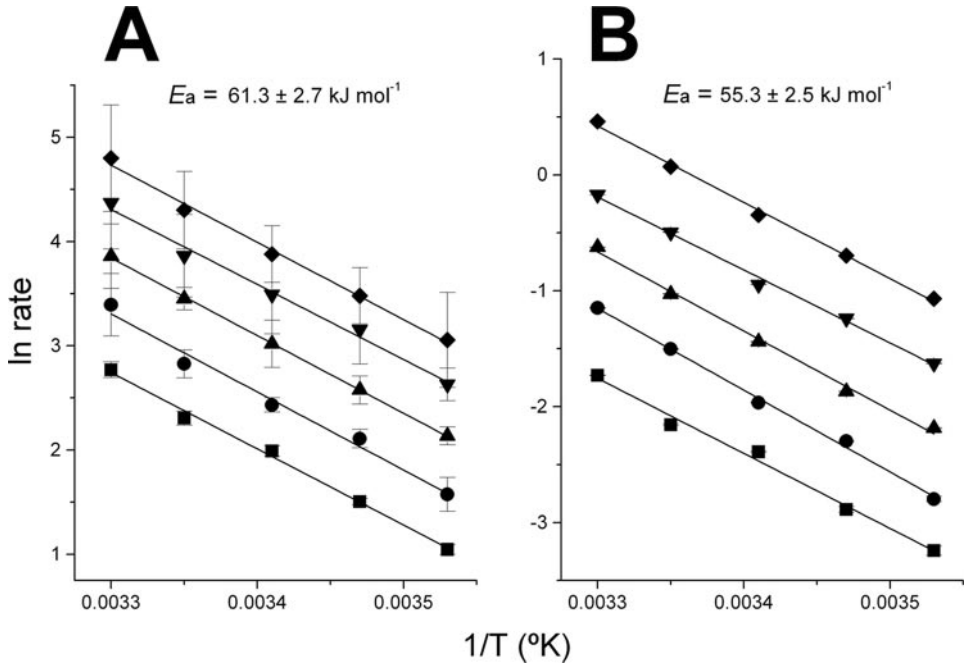

FIGURE 6. **Energy of activation for DBH_2 oxidation by the wild-type bc_1 complex.** Arrhenius plots show the initial rates of cytochrome *b* reduction (*A*) or the rates of the slow reduction of cytochrome *c* (*B*) at different temperatures obtained by rapid mixing of 10 μM cytochrome *c* and 1 μM wild-type bc_1 complex with DBH_2 at a concentration of 20 μM (■), 40 μM (●), 80 μM (▲), 160 μM (▼), or 320 μM (◆). *Error bars* correspond to the S.E. of the value of each rate after fitting of kinetic traces similar to those shown in Fig. 2 to the appropriate exponential function. Data points obtained at each DBH_2 concentration were fitted to a straight line, and the values of the corresponding slopes were averaged to obtain the indicated E_a value.

iting step appears, likely displaying a very different activation energy relative to the original slowest reaction. In the case of quinol oxidation at center P, it has been found that reduction of the Rieske protein is involved in the rate-limiting step (22, 32). In agreement with this conclusion, we observed a significantly higher E_a value for the bifurcated oxidation of DBH_2 in the Y185F bc_1 complex relative to the wild type (Table 1), which is due to a decreased difference in redox potential between quinol and the FeS cluster and thus decreased driving force for the bifurcated reaction.

In contrast, as shown in Table 1, the bifurcated reaction in the enzyme with the E272Q mutation exhibited a value of E_a identical to that of the wild-type enzyme. This result is in conflict with the hypothesis that substitution of Glu^{272} with a non-protonatable residue should impede movement of a semiquinone intermediate to a location

TABLE 1

Energy of activation (E_a) for the bifurcated and bypass oxidation of DBH_2 in bc_1 complexes with center P mutations

E_a values were calculated by averaging the slopes in Arrhenius plots obtained from the initial rate of cytochrome *b* reduction (bifurcated reaction) or the second slow phase of cytochrome *c* reduction (bypass reaction) by different concentrations of DBH_2, as shown in Fig. 6 for the wild-type enzyme.

bc_1 complex	E_a	
	Bifurcated	Bypass
	kJ mol^{-1}	
Wild-type	61.3 ± 2.7	55.3 ± 2.5
Y185F	72.9 ± 2.2	54.1 ± 3.8
E272Q	61.7 ± 3.0	52.2 ± 2.9
Y185F/E272Q	74.3 ± 1.4	56.3 ± 3.7

closer to the b_L heme, slowing down by orders of magnitude the rate of electron transfer to the heme (15) and consequently making this step slower than the reduction of the Rieske protein by quinol and thus rate-limiting. In the Y185F/E272Q double mutant enzyme, the E_a for the bifurcated oxidation of quinol was more difficult to determine because of the lower amount of enzyme obtained, the strong spectral contribution of cytochrome *c*, and the lower reduction extent of cytochrome *b*. Still, we were able to determine a value of ~74 kJ mol^{-1} (Table 1). Because this value was virtually identical to the one determined using the Y185F single mutant, it shows that in the E272Q mutant, the rate-limiting step was still linked to the redox potential of the Rieske protein and was not replaced by a supposedly slower electron transfer from semiquinone to the b_L heme.

The oxidation of quinol in the bypass reaction very likely involves a semiquinone intermediate, given that it involves the generation of a reductant strong enough to form superoxide (31). Interestingly, as shown in Table 1, the E_a for this process was unchanged relative to the wild type in both the Y185F and E272Q mutants, implying that the rate-limiting step for the semiquinone-mediated reduction of cytochrome *c* is clearly different from the one involved in the bifurcated oxidation of quinol, given the different dependence of the transition states of the two processes with respect to the midpoint potential of the Rieske protein. The E_a for the bypass reaction in the Y185F/E272Q double mutant was ~56 kJ mol^{-1}, close to the values obtained for each of the single mutants (Table 1) and much lower than the E_a for the bifurcated reaction (~74 kJ mol^{-1}).

DISCUSSION

Models for quinol oxidation that propose a sequential electron transfer have encountered the theoretical problem of how to account for a fast rate of electron transfer to the b_L heme from a semiquinone intermediate formed at a very low concentration (15). Mechanisms in which the semiquinone is stabilized (5) avoid the problem of having a low occupancy of this intermediate but have been disproved by the lack of detection of such a stable intermediate and by the observation that the slowest, rate-limiting step for quinol oxidation involves reduction of the Rieske protein (see Table 1) (15, 22, 32). A variant of the unstable semiquinone model has proposed that this species moves rapidly to the vicinity of the b_L heme (11), allowing a much faster, non-rate-limiting electron transfer even at very low semiquinone occupancies. Support for this hypothesis has been claimed from analysis of some crystallographic structures of the bc_1 complex in the presence of various inhibitors, which show two families of center P ligands that bind either distal or proximal to the b_L heme (11).

More recent crystallographic structures, however, cast doubt on the hypothetical movement of semiquinone to the proximal domain induced by rotation of Glu^{272}. Most of the inhibitors that occupy the distal domain of center P, including 5-*n*-heptyl-6-hydroxy-4,7-dioxobenzothiazole (13), 5-*n*-undecyl-6-hydroxy-4,7-dioxobenzothiazole, famoxadone, JG144, and NQNO (14), rotate the side chain of Glu^{272} away from the distal domain. Interestingly, all of these inhibitors structurally resemble quinol much more than those that bind to the proximal domain and have never been shown to bind promiscuously to both pockets of center P. Careful inspection of high-resolution structures also shows that the branched linear extensions of myxothiazol, MOA-stilbene, and azoxystrobin occupy the place of at least one water molecule (bonded to 5-*n*-heptyl-6-hydroxy-4,7-dioxobenzothiazole and the amino group of the Glu^{272} backbone in Fig. 1*B*) that probably aids in relaying the proximal proton of quinol to the membrane exterior. This implies that these proximal inhibitors block electron transfer to cytochrome *b* not by impeding movement of semiquinone (31) but by preventing one of the deprotonation events needed to form quinone.

Mutations at Glu^{272} have been shown to decrease the rate of quinol oxidation to almost the same rate as the bypass reactions (15). Most of these substitutions generate drastic conformational changes at center P, such as inducing resistance to myxothiazol, but not to stigmatellin (17), contrary to what would be expected from the binding of these inhibitors. However, the E272Q mutation, in which only an oxygen atom is replaced by a nitrogen, preserves the size of the side chain and induces resistance only to stigmatellin along with a slight decrease in substrate affinity (15, 16). Nevertheless, most substitutions at position 272 of cytochrome *b* inhibit the bifurcated oxidation of quinol only partially (15–17). One interpretation for this observation implies that a non-protonatable residue at position 272 prevents the movement of semiquinone to the vicinity of the b_L heme and that the partially inhibited rate results from electron tunneling from semiquinone in the position distal to the b_L heme (15). Because electron tunneling calculations imply a much slower electron transfer rate to b_L from the distal than from the proximal domain, reduction of the b_L heme by semiquinone would become slower than the formation of semiquinone. The consequences of this interpretation are illustrated in Fig. 7. Using the rates for the partial reactions included in the movable semiquinone model (15), the rate of quinol oxidation significantly decreases at semiquinone diffusion rates lower than 10^{11} s^{-1} (Fig. 7*A*), which are close to the proton exchange rate between hydrogen-bonded molecules. It is difficult to justify such high diffusion rates for semiquinone in view of the structural changes that would need to be involved, such as the displacement of entire sections of loops and helices in cytochrome *b* (11, 14) and the diffusion of the extrinsic domain of the Rieske protein, which has been calculated to be no faster than 10^8 s^{-1} (31).

The lower limit required for the rate of semiquinone diffusion to be non-rate-limiting comes from the very fast reverse rate of electron transfer from the Rieske FeS cluster back to

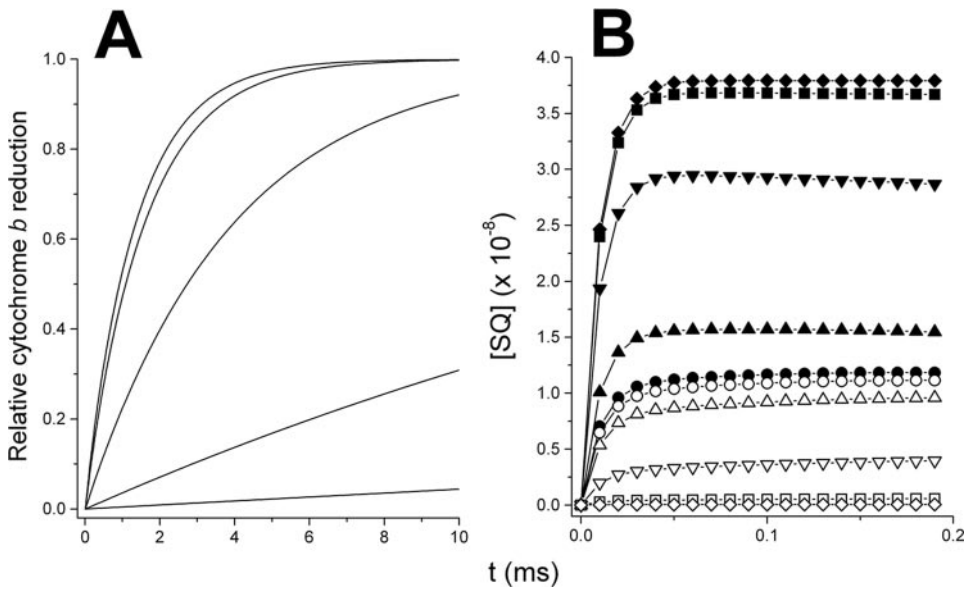

FIGURE 7. **Simulation of the kinetics of a sequential mechanism of quinol oxidation at center P.** Kinetics of cytochrome *b* reduction (*A*) and semiquinone concentration (*B*) were simulated using the rates described in the DynaFit model included as supplemental data. The diffusion rate constant for semiquinone movement from the distal to the proximal domain at center P was varied incrementally by one order of magnitude, from 10^{12} s^{-1} (fastest trace in *A*) to 10^{8} s^{-1} (slowest trace). The time-dependent change in concentration of semiquinone at the proximal (*closed symbols*) and distal (*open symbols*) positions shown in *B* were obtained using a semiquinone diffusion rate of 10^{12} s^{-1} (*circles*), 10^{11} s^{-1} (*triangles*), 10^{10} s^{-1} (*inverted triangles*), 10^{9} s^{-1} (*squares*), and 10^{8} s^{-1} (*diamonds*).

semiquinone to regenerate quinol. Based on a forward rate of 1.3×10^3 s^{-1} and a maximal semiquinone concentration of 4×10^{-8} at equilibrium (15), this reverse rate would be 3.25×10^{10} s^{-1}. Moreover, both the forward and reverse rates for the one-electron transfer between the Rieske cluster are probably greatly underestimated because they were calculated using the distance between quinol and the closest iron atom, instead of the much smaller distance to the FeS cluster ligand His^{181}, which should be considered as part of the electron conjugate system (35). In any case, diffusion of semiquinone would have to be significantly faster than the rate of reverse electron transfer from the Rieske cluster to semiquinone to allow a non-rate-limiting reduction of the b_L heme. At diffusion rates $<10^9$ s^{-1}, semiquinone would quickly reach its maximal equilibrium concentration at the distal position, and semiquinone would never reach the proximal domain before being re-reduced by the FeS cluster or oxidized by electron tunneling to the b_L heme (Fig. 7*B*). Under these conditions, quinol and the FeS cluster would be in rapid equilibrium relative to the slower electron transfer to b_L, and the first electron transfer that forms semiquinone at the distal domain would no longer be the rate-limiting step in the bifurcated reaction. Therefore, our results showing a lack of change of E_a in the E272Q enzyme with respect to the wild-type enzyme (see Table 1) indicate that the bifurcated oxidation of quinol does not proceed through a movable semiquinone mechanism (11). However, any sequential model in which an unstable semiquinone transfers its electron from the distal domain would still have to justify how to obtain fast rates to the b_L heme from an intermediate that exists at extremely low occupancies (15).

As Berry and Huang (35) have proposed, a mechanism in which electron transfer proceeds from a quinol-imidazolate-FeS electron donor complex that exists at full occupancy under conditions of substrate saturation would circumvent the theoretical problems presented by sequential models. In this mechanism, electronic coupling between the three bonded partners in the donor complex would effectively delocalize one electron from quinol over the entire conjugate, with no formal valence change in the FeS cluster or formation of an actual semiquinone intermediate. The bifurcated electron transfer reaction, resulting in a simultaneous formal valence change in both the FeS cluster and the b_L heme, would proceed from the donor complex only when a proton acceptor is available in cytochrome *b*. The immediate acceptor in substrate deprotonation is probably a water molecule hydrogen-bonded to the carboxylate of Glu^{272} (see Fig. 1*A*), as is predicted by molecular modeling of the binding of hydroxynaphthoquinone inhibitors at center P (36). In the E272Q enzyme, the affinity of this water molecule for the proton in quinol would be reduced, but not completely abolished, explaining the partial inhibition of the bifurcated reaction by mutations in Glu^{272} (15–17). The distribution of the delocalized electron within the donor complex, determined by the E_m of the FeS cluster, would dictate the activation energy for the bifurcated electron transfer, as well as the ability to donate a proton. The electron and the proton from the donor complex do not tunnel to the same acceptor together, given that the b_L heme only receives the electron, whereas the proton is donated to either a water molecule or to the Glu^{272} carboxylate. Therefore, reduction of the b_L heme is not a proton coupled-electron transfer event, and the activation energy for reduction of the b_L heme depends only on the driving force determined by the difference in redox potentials between the donor complex and the heme. However, the rate of reduction of the b_L heme is also affected by the probability of the donor complex to become deprotonated. The synergistic decrease in the bifurcated rate observed in the Y185F/E272Q mutant (see Fig. 5) probably reflects an increase in the proton affinity of the electron donor complex when the Rieske redox potential is lowered. Because this proton must be removed from the donor complex for formation of the quinone product, the electron transfer to the b_L heme also becomes less likely than in the E272Q mutant that has a normal E_m value for the FeS cluster. Such a synergistic effect is difficult to explain in the context of a sequential mechanism in which the two-electron transfer steps from quinol and semiquinone are considered as separate reactions.

The fact that the bypass reaction is much slower than the bifurcated oxidation of quinol indicates that both processes do not have the same rate-limiting step; otherwise, they would, by

definition, have the same rate. A previous study using steady state kinetics in submitochondrial particles (32) concluded that the activation energies for the bifurcated and bypass reaction were similar, although a statistically significant difference of ~3.5 kJ mol^{-1} (higher for the bypass reaction) was found between the two processes at pH 8. We have now found a larger difference of ~6 kJ mol^{-1} at pH 7 (see Fig. 6) with the bypass reaction showing a lower E_a. Our present pre-steady state conditions eliminate the interference of the non-enzymatic reduction of cytochrome *c* by DBH_2, in contrast with the previous work (32), where the chemical reaction was relatively much larger and was corrected only by measuring rates before the addition of the enzyme mixed with phospholipids, which are likely to enhance the chemical reaction. Because a statistically significant difference in the E_a of the bypass reaction between the wild type and mutants with a lower Rieske protein potential was found only for the very slow S183A enzyme (32), it is likely that an error in the correction for the chemical reaction (which should have a higher E_a than the enzymatically catalyzed process) gave an overestimated E_a value in this mutant.

In the present work, we have found no influence of the Rieske redox potential on the E_a value of the bypass reaction, confirming that this process does not share the same rate-limiting step as the bifurcated reaction (see Table 1). This provides further support to the conclusion that quinol oxidation is a concerted process that does not proceed through a semiquinone intermediate. Only when the cytochrome *b* acceptors for the electron or the proton are unavailable at center P would formation of semiquinone occur, mainly by reactions that are irrelevant to the bifurcated mechanism, such as the reverse electron transfer from the b_L heme to quinone (37). The fact that one can force the bc_1 complex to generate a semiquinone radical under artificial conditions is not proof that a semiquinone is normally an intermediate in the ubiquinol oxidation reaction at center P. Therefore, the unstable semiquinone radicals that have been generated at center P under inhibited conditions (9, 10) should not be considered as evidence supporting any sequential mechanism for the oxidation of quinol in the bc_1 complex.

REFERENCES

1. Mitchell, P. (1976) *J. Theor. Biol.* **62,** 327–367
2. Trumpower, B. L., and Gennis, R. B. (1994) *Annu. Rev. Biochem.* **63,** 675–716
3. Osyczka, A., Moser, C. C., Daldal, F., and Dutton, P. L. (2004) *Nature* **427,** 607–612
4. Zhu, J., Egawa, T., Yeh, S. R., Yu, L., and Yu, C. A. (2007) *Proc. Natl. Acad. Sci. U. S. A.* **104,** 4864–4869
5. Link, T. A. (1997) *FEBS Lett.* **412,** 257–264
6. Crofts, A. R., and Wang, Z. (1989) *Photosynth. Res.* **22,** 69–87
7. Rich, P. R. (2004) *Biochim. Biophys. Acta* **1658,** 165–171
8. Cape, J. L., Bowman, M. K., and Kramer, D. M. (2005) *J. Am. Chem. Soc.* **127,** 4208–4215
9. Cape, J. L., Bowman, M. K., and Kramer, D. M. (2007) *Proc. Natl. Acad. Sci. U. S. A.* **104,** 7887–7892
10. Zhang, Z., Osyczka, A., Dutton, P. L., and Moser, C. C. (2007) *Biochim. Biophys. Acta* **1767,** 883–887
11. Crofts, A. R., Barquera, B., Gennis, R. B., Kuras, R., Guergova-Kuras, M., and Berry, E. A. (1999) *Biochemistry* **38,** 15807–15826
12. Hunte, C., Koepke, J., Lange, C. Rossmanith, T., and Michel, H. (2000) *Structure* (*Camb.*) **8,** 669–684
13. Palsdottir, H., Lojero, C. G., Trumpower, B. L., and Hunte, C. (2003) *J. Biol. Chem.* **278,** 31303–31311
14. Esser, L. Gong, X., Yang, S., Yu, L., Yu, C. A., and Xia, D. (2006) *Proc. Natl. Acad. Sci. U. S. A.* **103,** 13045–13050
15. Crofts, A. R., Lhee, S., Crofts, S. B., Cheng, J., and Rose, S. (2006) *Biochim. Biophys. Acta* **1757,** 1019–1034
16. Wenz, T., Hellwig, P., MacMillan, F., Meunier, B., and Hunte, C. (2006) *Biochemistry* **45,** 9042–9052
17. Seddiki, N., Meunier, B., Lemesle-Meunier, D., and Brasseur, G. (2008) *Biochemistry* **47,** 2357–2368
18. Trumpower, B. L., and Edwards, C. A. (1979) *J. Biol. Chem.* **254,** 8697–8706
19. Rich, P. R. (1984) *Biochim. Biophys. Acta* **768,** 53–79
20. Gutierrez-Cirlos, E. B., Merbitz-Zahradnik, T., and Trumpower, B. L. (2002) *J. Biol. Chem.* **277,** 1195–1202
21. Von Jagow, G., and Link, T. A. (1986) *Methods Enzymol.* **126,** 253–271
22. Denke, E., Merbitz-Zahradnik, T., Hatzfeld, O. M., Snyder, C. H., Link, T. A., and Trumpower, B. L. (1998) *J. Biol. Chem.* **273,** 9085–9093
23. Ljungdahl, P. O., Pennoyer, J. D., Robertson, D. E., and Trumpower, B. L. (1987) *Biochim. Biophys. Acta* **891,** 227–241
24. Snyder, C. H., and Trumpower, B. L. (1998) *Biochim. Biophys. Acta* **1365,** 125–134
25. Yu, C. A., Yu, L., and King, T. E. (1972) *J. Biol. Chem.* **247,** 1012–1019
26. Berden, J. A., and Slater, E. C. (1970) *Biochim. Biophys. Acta* **216,** 237–249
27. Covian, R., Gutierrez-Cirlos, E. B., and Trumpower, B. L. (2004), *J. Biol. Chem.* 15040–15049
28. Margoliash, E., and Walasek, O. F. (1967) *Methods Enzymol.* **10,** 339–348
29. Kuzmic, P. (1996) *Anal. Biochem.* **237,** 260–273
30. Covian, R., Kleinschroth, T., Ludwig, B., and Trumpower, B. L. (2007) *J. Biol. Chem.* **282,** 22289–22297
31. Muller, F., Crofts, A. R., and Kramer, D. M. (2002) *Biochemistry* **41,** 7866–7874
32. Forquer, I., Covian, R., Bowman, M. K., Trumpower, B. L., and Kramer, D. M. (2006) *J. Biol. Chem.* **281,** 38459–38465
33. Helenius, A., and Simons, K. (1975) *Biochim. Biophys. Acta* **415,** 29–79
34. Humphreys, K. J., and Rhodes, C. T. (1968) *J. Pharm. Sci.* **57,** 79–83
35. Berry, E. A., and Huang, L. S. (2003) *FEBS Lett.* **555,** 13–20
36. Kessl, J. J., Moskalev, N. V. Gribble, G. W., Nasr, M., Meshnick, S. R., and Trumpower, B. L. (2007) *Biochim. Biophys. Acta* **1767,** 319–326
37. Drose, S., and Brandt, U. (2008) *J. Biol. Chem.* **283,** 21649–21654